한국소음진동공학회논문집 제 17 권 제 5 호, pp. 415~426, 2007.

Dynamic Balancing in a Link Motion Punch Press
링크모션 펀치프레스의 다이나믹 발란싱

Jin Sung Suh†
서 진 성

(Received January 21, 2007 ; Accepted April 3, 2006)

Key Words : Dynamic Balancing(동적발란싱), Link Motion Mechanism(링크모션 메커니즘), Constraint Joint (구속조인트), Constraint Equation(구속방정식), spm(Strokes per minute)

ABSTRACT

In a link motion punch press, numerous links are interconnected and each link executes a constrained motion at high speed. As a consequence, dynamic unbalance force and moment are transmitted to the main frame of the press, which results in unwanted vibration. This degrades productivity and precise stamping work of the press. This paper presents an effective method for reducing dynamic unbalance in a link motion punch press based upon kinematic and dynamic analyses. Firstly, the kinematic analysis is carried out in order to understand the fundamental characteristics of the link motion mechanism. Then design variable approach is presented in order to automate the model setup for the mechanism whenever design changes are necessary. To obtain the inertia properties of the links such as mass, mass moment of inertia, and the center of mass, 3-dimensional CAD software was utilized. Dynamic simulations were carried out for various combinations of design changes on some links having significant influences on kinematic and dynamic behavior of the mechanism.

요 약

링크모션 펀치프레스는 많은 링크들이 서로 연결되어 있으며 각각의 링크는 고속에서 구속운동을 수행한다. 그 결과 동적 불평형 힘과 모멘트가 프레스의 메인프레임으로 전달되며 원하지 않는 진동을 수반한다. 이로 인하여 생산성과 정확한 스탬핑 작업의 저하를 초래한다. 이 논문은 기구학 및 동역학 분석에 기초하여 링크모션 펀치프레스의 다아나믹 언발란스를 저감하는 효과적인 방법을 제시한다. 그리고 디자인 변화가 필요할 때마다 메커니즘의 모델 구성을 자동화하기 위한 디자인 변수 방식을 소개한다. 질량, 질량관성모멘트, 질량중심 등의 링크들의 관성 성질을 얻기 위하여 3차원 캐드 소프트웨어를 활용하였다. 메커니즘의 기구학적, 동역학적 거동에 주요한 영향을 미치는 일부 링크들의 디자인을 변화시킬 때 얻을 수 있는 다양한 조합에 대하여 동역학 시뮬레이션을 수행하였다.

1. Introduction

When the links comprising a link motion punch press are executing constrained motions, time-varying forces and moments are transmitted to the main frame of the press, which produce vibration. These force and moment are called dynamic unbalance force and moment. They are

† Corresponding Author : Member, Department of Mechanical Engineering, Korea Polytechnic Univ.
E-mail : jssuh@kpu.ac.kr
Tel : (031) 8041-0408, Fax : (031) 8041-0419

transmitted to the main frame at the locations on the main frame where the kinematic constraint joints, which connect some links to the main frame, are defined. Therefore dynamic balancing is the technique minimizing dynamic unbalance force and moment.

Many studies have been undertaken on balancing planar and spatial mechanisms. The general technique for dynamic balancing is to make the overall mass center of a mechanism as stationary as possible by using counterweights[1~5]. This is actually equivalent to the technique of reducing the resultant dynamic unbalance force and moment transmitted to the main frame of the mechanism, which is presented in this work. Another important technique also in wide use is to make the total potential energy of a mechanism constant by using springs[6~9]. Arakelian and Smith presented a review of the balancing techniques by counterweights and harmonic balancing by two counter-rotating masses[10]. Ouyang and Zhang introduced a new force balancing method of adjusting kinematic parameters for robotic mechanisms as opposed to force balancing methods using counterweights[11]. In automotive applications Kim et. al. presented a technique for designing a balance shaft module[12]. Real mechanisms in high speed operation, however, exhibit some flexibility due to elasticity and some plasticity. To account for these real-life phenomena the techniques dealing with elastic and even plastic deformations of the flexible multibody systems have been developed[13~15]. Furthermore, there exist some clearances in each kinematical joint, and this will lead to collision and wear. A methodology for including the effects of the inherent clearances and lubrications in multibody mechanical systems have also been developed[16,17]. The incorporation of all these real-life effects into the model of a link motion punch press will produce more realistic results when the problems such as heavy computational burden and modeling complexities are resolved.

In this work, all the links in a link motion mechanism are assumed to be rigid, and a method for balancing a complicated link motion mechanism is presented. Firstly, kinematic motions of the mechanism are analyzed. In a link motion punch press, a pair of counterbalance weights is used in order to counteract the dynamic unbalance force and moment. Focusing on the kinematic relationships between the counterbalance weights and other links, optimal kinematic conditions are studied for achieving best dynamic balancing.

In order to automate the setup of the model for the mechanism whenever some design changes are required, some important aspects of the mechanism such as link lengths, locations of joint constraints were assigned as design variables.

Dynamic unbalance force and moment are formulated by using both Newtonian and Lagrangian mechanics. Although they produce identical dynamic simulation results, they have their own merits and demerits.

In Newtonian mechanics, the inertia force and inertia moment of each moving link can be directly computed when its center-of-mass acceleration and angular acceleration are known. The inertia force and inertia moment of every link is added up respectively, in order to produce the resultant dynamic unbalance force and moment[18]. This means that only kinematical information is needed and the computational burden will be greatly relieved compared to Lagrangian mechanics. However, the joint reaction forces and moments cannot be obtained from pure kinematical information. In order to obtain these, the Newtons second law of motion should be applied to every individual link and solved simultaneously, which is quite a formidable task.

In Lagrangian mechanics, the vectors of Lagrange multipliers and constraint equations are used to compute the joint reaction forces and moments acting on the constraint joints defined on the main frame. From these, dynamic unbalance force and moment can be obtained[19]. This gives extra computational burden compared to Newtonian mechanics, but provides valuable information on dynamic loading acting on each constraint joint.

All the links were designed by utilizing a 3-D CAD software. From this, inertia properties of each link such as mass, mass moment of inertia, location of the center of mass could be obtained. Design changes on some links including the counterbalance weights have significant effects on dynamic balancing of the whole mechanism. For many possible combinations of design variations in the mechanism, kinematic and dynamic simulations were carried out during a single rotation of the crank shaft in order to reduce dynamic unbalance.

2. Analysis of Link Motion Mechanism

2.1 Description of Motion of the Mechanism Associated with Dynamic Balancing

In Fig. 1, the kinematic model of a link motion punch press is shown. The mechanism executes a 2 dimensional plane motion. And the press is assumed to be operated at 1,200 spm. This means that the crankshaft is being driven at 1,200 revolutions per minute with constant angular velocity. In Table 1, the names, lengths, and numerical symbols for mass centers are presented regarding the links shown in Fig. 1. For example, $Link_{0,2}$ represents the link connecting points ⓪ and ②, and it is named as crankshaft. The length between the points ⓪ and ② is the eccentricity of the crankshaft and will be denoted as ε_{crank} in this work. The rotation center of crankshaft is denoted as point

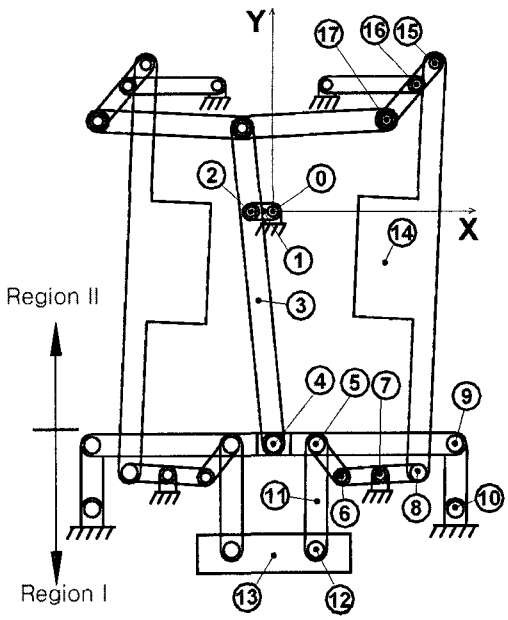

Fig. 1 Model of the mechanism of a link motion punch press

Table 1 Names of each link and location shown in Fig. 1 with link length in brackets. Numerical values for lengths given in parentheses are fixed throughout this work

Symbol for each link and location	Name
$Link_{0,2}$	Crankshaft
⓪	Rotation center of $Link_{0,2}$
①	c.m. of $Link_{0,2}$
$Link_{2,4}$	Connecting rod(300 mm)
③	c.m.[1] of $Link_{2,4}$
$Link_{4,9}$	Main lever(470 mm)
$Link_{5,6}$	Eccentric link
$Link_{6,8}$	Lifting lever(276 mm)
$Link_{9,10}$	Die-height adjust lever(130 mm)
$Link_{8,15}$	Counterbalance weight(614 mm)
$Link_{15,17}$	Pivoting lever
$Link_{5,12}$	Slide column(471 mm)
⑪	c.m. of slide column
⑬	c.m. of slide
⑭	c.m. of counterbalance weight

[1]c.m.: Center of mass

⓪. A Newtonian inertial frame of reference (OXY) is fixed to the main frame with its origin O coinciding with point ⓪. Points ④ and ⑬ are constrained to move only in vertical direction. The model of the mechanism shown in Fig. 1 has 23 links in total including the ground link, which is the main frame. The main frame is depicted as hatched lines as shown in Fig. 1. Be aware that there is an additional link in the form of a long circular bar, which penetrates through $Link_{2,4}$ and $Link_{4,9}$ at point ④ into the normal direction of the plane of the paper. There also exists a vertical prismatic joint between a long circular bar and the main frame. This long circular bar can possibly be named as crossover.

To counteract dynamic unbalance a pair of counterbalance weights is used as shown in Fig. 1. The design of a vibration isolation system on which the press is mounted is important as well[18,20]. The total mass of the press including all the moving links, the main frame, and other accessories is approximately 7,500 kg.

In Fig. 1, for all the links located in Region I, a pair of identical links in the left-hand and right-hand sides of the Y axis, executes motions which are symmetric with respect to the Y axis. Therefore, their resultant inertia force in X direction is 0, and their resultant inertia moment in Z direction is also 0. Therefore all the links located in Region I transmit only the resultant inertia force in Y direction to the main frame. For efficiently counteracting the unbalance force in Y direction, the orientation of $Link_{5,6}$ should remain as vertical as possible, and those of $Link_{4,9}$ and $Link_{6,8}$ as horizontal as possible during one revolution of the crankshaft. This will be demonstrated later in Fig. 4. $Link_{5,6}$ and $Link_{6,8}$ in Fig. 1, however, are intentionally drawn in oblique directions in order to represent the mechanism in its most general form. Also an intention was to avoid cluttering up the drawing since the length of $Link_{5,6}$ is, in general practice, about 1/17 of that of $Link_{6,8}$ as presented in Table 1 and Table 2.

The resultant inertia force in X direction and resultant inertia moment in Z direction produced by the links located in Region II excluding the counterbalance weights should be counteracted by the counterbalance weights. For achieving this efficiently, the orientation of $Link_{5,6}$ should remain as vertical as possible, and those of $Link_{4,9}$ and $Link_{6,8}$ as horizontal as possible during one revolution of the crankshaft as mentioned previously. This will be demonstrated later in Fig. 4. The point ⑯ acts as a pivot for $Link_{15,17}$. When the length $l_{15,17}$ of $Link_{15,17}$ is held fixed, increasing the length $l_{15,16}$ between points ⑮ and ⑯ increases the amplitudes of the components of the accelerations in X direction of the mass centers of the counterbalance weights. The same is true of the angular accelerations in Z direction of the counterbalance weights.

2.3 Kinematic Analysis of the Mechanism

The mechanism shown in Fig. 1 is kinematically driven since the number of linearly independent constraint equations is equal to the number of the system generalized coordinates. One of the constraint equations is the driving constraint equation prescribed for constant angular velocity of the crankshaft. In this work, the crankshaft is driven at 1,200 rpm with constant angular velocity. Therefore the mechanism has zero degrees of freedom.

At each specified angular position of the crankshaft, the linear and angular positions of the links can be obtained by solving the vector of the constraint equations given by[19]

$$\boldsymbol{C}(\mathbf{q},t)=[C_1(\mathbf{q},t)\ C_2(\mathbf{q},t)\cdots C_n(\mathbf{q},t)]^T=\mathbf{0} \qquad (1)$$

where n is the number of system generalized

coordinates $\mathbf{q}$ which is given by

$$\mathbf{q} = [q_1 \; q_2 \cdots q_n]^T \tag{2}$$

After differentiating the vector of the constraint equations with respect to time, the generalized velocity vector $\dot{\mathbf{q}}$ can be evaluated by solving

$$\mathbf{C}_q \dot{\mathbf{q}} + \mathbf{C}_t = \mathbf{0} \tag{3}$$

where $\mathbf{C}_q$ is the constraint Jacobian matrix, $\mathbf{C}_t$ is the vector of partial derivative of the constraint equations with respect to time.

Differentiating Eq. (3) with respect to time, the generalized acceleration vector $\ddot{\mathbf{q}}$ can be evaluated by solving

$$\mathbf{C}_q \ddot{\mathbf{q}} = -(\mathbf{C}_q \dot{\mathbf{q}})_q \dot{\mathbf{q}} - 2\mathbf{C}_{qt} \dot{\mathbf{q}} - \mathbf{C}_{tt} \tag{4}$$

where $\mathbf{C}_{qt}$ is the matrix of partial derivative of the constraint Jacobian matrix with respect to time, and $\mathbf{C}_{tt}$ is the vector of partial derivative of $\mathbf{C}_t$ with respect to time.

2.3 Automation of Mechanism Design

When the link lengths or the locations of constraint joints vary, the model of the whole mechanism should be reconstructed from the beginning. Then new kinematic and dynamic analyses of the mechanism should be followed. For example in Fig. 1, when the die height increases by 30 mm, the slide should be raised by 30 mmm. For this, point ⑩ should be raised in vertical direction approximately by 75 mm in this work. This will result in a substantial change in the structure of the mechanism. Its kinematic and dynamic characteristics also change substantially.

If the lengths of some links or the coordinates of constraint joints can be assigned as design variables, then the model setup of the mechanism can be automated and its kinematic and dynamic analyses can be carried out immediately after design changes. All the x and y coordinates in this section are given with respect to the Newtonian inertial frame of reference.

Let us assign the eccentricity of the crankshaft and the length of the connecting rod as design variables, and let their names be ε_{crank} and l_{con_rod}, respectively. Then the y coordinate of point ④, y_4, is given by

$$y_4 = -\sqrt{l_{con\_rod}^2 - \varepsilon_{crank}^2} \tag{5}$$

Next, let the x and y coordinates of point be assigned as design variables x_{10} and y_{10}, respectively. Also let the lengths of $Link_{4,9}$ and $Link_{9,10}$ be assigned as design variables $l_{4,9}$ and $l_{9,10}$. Point ⑩ is the location where a revolute joint is defined which connects $Link_{9,10}$ to the main frame. Then x_9 and y_9 are given by

$$x_9 = x_{10} - l_{9,10} \times cos\left\{ \begin{array}{l} tan^{-1}\dfrac{y_4 - y_{10}}{x_{10}} + \\ cos^{-1}\left(\dfrac{l_{4,10}^2 + l_{9,10}^2 - l_{4,9}^2}{2 \cdot l_{4,10} \cdot l_{9,10}} \right) \end{array} \right\} \tag{6}$$

$$y_9 = y_{10} + l_{9,10} \times sin\left\{ \begin{array}{l} tan^{-1}\dfrac{y_4 - y_{10}}{x_{10}} + \\ cos^{-1}\left(\dfrac{l_{4,10}^2 + l_{9,10}^2 - l_{4,9}^2}{2 \cdot l_{4,10} \cdot l_{9,10}} \right) \end{array} \right\} \tag{7}$$

Point ⑤ lies on a straight line connecting the end points ④ and ⑨ of $Link_{4,9}$. Also are volute joint is defined at Point ⑤. The distance $l_{4,5}$ between points ④ and ⑤ can be assigned as a design variable, then the x and y coordinates x_5, y_5 of point will be given by

$$x_5 = \frac{l_{4,5}}{l_{4,9}} \cdot x_9 \tag{8}$$

$$y_5 = y_4 + \frac{l_{4,5}}{l_{4,9}} \cdot (y_9 - y_4) \tag{9}$$

Let the x and y coordinates x_7, y_7 of point ⑦, lengths $l_{5,6}$ and $l_{6,8}$ of Link$_{5,6}$ and Link$_{6,8}$ be assigned as design variables. Point ⑦ is assumed to be the midpoint of Link$_{6,8}$. Then the x and y coordinates x_6, y_6 of point ⑥ will be given by

$$x_6 = x_5 + l_{5,6} \times \cos\left\{ \begin{array}{l} \tan^{-1}\dfrac{y_5 - y_7}{x_7 - x_5} + \\ \cos^{-1}\left(\dfrac{l_{5,7}^2 + l_{5,6}^2 - (l_{6,8}/2)^2}{2 \cdot l_{5,7} \cdot l_{5,6}} \right) \end{array} \right\} \tag{10}$$

$$y_6 = y_5 - l_{5,6} \times \sin\left\{ \begin{array}{l} \tan^{-1}\dfrac{y_5 - y_7}{x_7 - x_5} + \\ \cos^{-1}\left(\dfrac{l_{5,7}^2 + l_{5,6}^2 - (l_{6,8}/2)^2}{2 \cdot l_{5,7} \cdot l_{5,6}} \right) \end{array} \right\} \tag{11}$$

The x and y coordinates x_8, y_8 of point will be given by

$$x_8 = 2x_7 - x_6 \tag{12}$$

$$y_8 = 2y_7 - y_6 \tag{13}$$

By repeating these procedures, the model setup of the whole mechanism can be automated. Of course, the coordinates of the constraint joints should satisfy the corresponding constraint equations in Eq. (1).

3. Dynamic Balancing

3.1 Theory of Dynamic Balancing by Newtonian Mechanics

When the Newton's laws are applied to a mechanism consisting of n_b moving links, the following relations can be derived[18].

$$\mathbf{P}^{(e)} + \mathbf{\Phi} + \mathbf{R}^{(e)} = \mathbf{0} \tag{14}$$

$$\mathbf{M}_O^{(P_e)} + \mathbf{M}_O^{(\Phi)} + \mathbf{M}_O^{(R_e)} = \mathbf{0} \tag{15}$$

Where $\mathbf{P}^{(e)}$ is the vector sum of the external forces acting on n_b links, and in the case of the press it is 0 since there is no external force. $\mathbf{\Phi}$ is the vector sum of the inertia forces which n_b links have. $\mathbf{R}^{(e)}$ is the vector sum of the joint reaction forces which are applied to n_b links by the main frame, and the points of application of these forces are the constraint joints defined on the main frame. $\mathbf{M}_O^{(P_e)}$ is the vector sum of the moments of the external forces acting on n_b links with respect to the rotation center of the crankshaft. For the case of a link motion punch press, when a moment is applied to the crankshaft by a motor which is fixed to the mainframe, are action moment which is of the same magnitude but in opposite direction is also applied to the main frame through the stator of a motor. These constitute a pair of internal moments for the press as a whole. Therefore, $\mathbf{M}_O^{(P_e)}$ is also 0. $\mathbf{M}_O^{(\Phi)}$ is the vector sum of the inertia moments of n_b links with respect to the rotation center of the crankshaft. $\mathbf{M}_O^{(R_e)}$ is the vector sum of the moments of the joint reaction forces acting on n_b links with respect to the rotation center of the crankshaft.

According to the Newton's third law, the dynamic unbalance force $\mathbf{F}_{U.B.}$ is equal to $-\mathbf{R}^{(e)}$, and also equal to $\mathbf{\Phi}$ according to Eq. (14). Likewise the dynamic unbalance moment $\mathbf{M}_{U.B.}$ taken with respect to the rotation center of the crankshaft is equal to $-\mathbf{M}_O^{(R_e)}$, and also equal to $\mathbf{M}_O^{(\Phi)}$ according to Eq. (15). These relations can be summarized as

$$\mathbf{F}_{U.B.} = -\mathbf{R}^{(e)} = \mathbf{\Phi} \tag{16}$$

$$\mathbf{M}_{U.B.} = -\mathbf{M}_O^{(R_e)} = \mathbf{M}_O^{(\Phi)} \tag{17}$$

Dynamic balancing is the work reducing $\mathbf{F}_{U.B}$ and $\mathbf{M}_{U.B.}$

3.2 Theory of Dynamic Balancing by Lagrangian Mechanics

The generalized acceleration vector $\ddot{\mathbf{q}}$ and

the vector of Lagrange multipliers $\boldsymbol{\lambda}$ can be obtained by solving[19]

$$\begin{bmatrix} \mathbf{M} & \mathbf{C}_q^T \\ \mathbf{C}_q & \mathbf{0} \end{bmatrix} \begin{bmatrix} \ddot{\mathbf{q}} \\ \boldsymbol{\lambda} \end{bmatrix} = \begin{bmatrix} \mathbf{Q}_e \\ \mathbf{Q}_d \end{bmatrix} \tag{18}$$

where $\mathbf{M}$ is the system mass matrix. $\mathbf{Q}_e$ is the vector of system generalized external forces, and is 0 for the case of the press. From Eq. (4) $\mathbf{Q}_d$ is given by

$$\mathbf{Q}_d = -(\mathbf{C}_q \dot{\mathbf{q}})_q \dot{\mathbf{q}} - 2\mathbf{C}_{qt}\dot{\mathbf{q}} - \mathbf{C}_{tt} \tag{19}$$

The vectors of the system generalized constraint forces, $\mathbf{Q}_c$, and $\boldsymbol{\lambda}$ satisfy the following relation

$$\mathbf{Q}_c = -\mathbf{C}_q^T \boldsymbol{\lambda} \tag{20}$$

The solution of Eq. (18) is given by

$$\begin{aligned} \ddot{\mathbf{q}} &= \mathbf{H}_{qq}\mathbf{Q}_e + \mathbf{H}_{q\lambda}\mathbf{Q}_d = \mathbf{H}_{q\lambda}\mathbf{Q}_d \\ \boldsymbol{\lambda} &= \mathbf{H}_{\lambda q}\mathbf{Q}_e + \mathbf{H}_{\lambda\lambda}\mathbf{Q}_d = \mathbf{H}_{\lambda\lambda}\mathbf{Q}_d \end{aligned} \tag{21}$$

where

$$\begin{aligned} \mathbf{H}_{\lambda\lambda} &= (\mathbf{C}_q\mathbf{M}^{-1}\mathbf{C}_q^T)^{-1} \\ \mathbf{H}_{qq} &= \mathbf{M}^{-1} + \mathbf{M}^{-1}\mathbf{C}_q^T\mathbf{H}_{\lambda\lambda}\mathbf{C}_q\mathbf{M}^{-1} \\ \mathbf{H}_{q\lambda} &= \mathbf{H}_{\lambda q}^T = -\mathbf{M}^{-1}\mathbf{C}_q^T\mathbf{H}_{\lambda\lambda} \end{aligned} \tag{22}$$

To obtain the dynamic unbalance force and moment applied to the main frame, the joint reaction forces and moments acting on the constraint joints defined on the main frame should be obtained first. When link i is connected to the main frame by a given joint k, the generalized constraint forces acting on link i is given by

$$(\mathbf{Q}_c^i)_k = -(\mathbf{C}_k)_{\mathbf{q}^i}^T \boldsymbol{\lambda}_k = [F_{xk}^i \quad F_{yk}^i \quad M_k^i]^T \tag{23}$$

where F_{xk}^i F_{yk}^i M_k^i are the components of the vector $(\mathbf{Q}_c^i)_k$ and they are defined with respect to a local coordinate system which is attached to link i. The origin of the local coordinate system coincides with the mass center of link i. $\mathbf{C}_k$ is the vector of constraint equations of joint k, $\boldsymbol{\lambda}_k$ is the vector of Lagrange multipliers associated with $\mathbf{C}_k$.

Let $\mathbf{u}_p^i$ be the position vector from the origin of the local coordinate system of link i to joint k. Then the vector of the actual joint reaction forces and moment, $\mathbf{F}^i$, is given by

$$\mathbf{F}^i = [F_{xk}^i \quad F_{yk}^i \quad M_k^i - (\mathbf{u}_p^i \times \mathbf{F}_k^i)\cdot\mathbf{k}]^T \tag{24}$$

where $\mathbf{F}_k^i = [F_{xk}^i \quad F_{yk}^i]^T$, and $\mathbf{k}$ is a unit vector along the axis of rotation. Then the moment $(M_k^i)_O$ with respect to the rotation center of the crankshaft is given by

$$(M_k^i)_O = M_k^i - (\mathbf{u}_p^i \times \mathbf{F}_k^i)\cdot\mathbf{k} + (\mathbf{R}_k \times \mathbf{F}_k^i)\cdot\mathbf{k} \tag{25}$$

$\mathbf{R}_k$ is the position vector from the rotation center of the crankshaft to joint k.

The dynamic unbalance force, $\mathbf{F}_{U.B.}$, and the dynamic unbalance moment, $\mathbf{M}_{U.B.}$, which are transmitted to the main frame, are given by

$$\mathbf{F}_{U.B.} = -\sum_{k,i} \mathbf{F}_k^i \tag{26}$$

$$\mathbf{M}_{U.B.} = -\left\{\sum_{k,i} (M_k^i)_O\right\}\mathbf{k} \tag{27}$$

3.3 Results of Dynamic Balancing

The sequential procedure of changing the design variables for reaching satisfactory dynamic balancing is summarized below.

(1) When the orientation of the crankshaft, $\text{Link}_{0,2}$, is horizontal as shown in Fig. 1, the orientation of $\text{Link}_{5,6}$ should be close to vertical, and those of $\text{Link}_{4,9}$ and $\text{Link}_{6,8}$ beclose to horizontal.

(2) When the orientation of the crankshaft is vertical, those of a pair of counterbalance

weights, $Link_{8,15}$ and the one on the left-hand side, should be close to vertical.

(3) Firstly, try to reduce the component of the resultant dynamic unbalance force in Y-direction. Until the required level of the resultant unbalance force is reached, keep running dynamic simulations by trimming excess mass from or adding additional masses on the counterbalance weights, i.e. by shaping them by a 3-D CAD software. After each shaping, the mass, the moment of inertia, and the mass center of a counterbalance weight change.

(4) Secondly, try to reduce both the component of the resultant dynamic unbalance force in X-direction and the resultant unbalance moment in Z-direction. This can be done by varying the ratio between the length $l_{15,16}$ and the length $l_{16,17}$.

(5) If the results are not successful, repeat (3) and (4) again.

Table 2 Design parameters before and after dynamic balancing

	Before balancing	After balancing
Crankshaft eccentricity : e_{crank}	20.90 mm	20.87 mm
$l_{4,5}$	188.20 mm	188.00 mm
$l_{5,6}$	15.60 mm	16.00 mm
Position of ⑦ (in mm)	(325.0, -314.0, 0.0)	(325.0, -313.0, 0.0)
Position of ⑩ (in mm)	(460.0, -348.9, 0.0)	(460.0, -427.1, 0.0)
Stroke[1]	25.00 mm	25.04 mm
Orientation of $Link_{4,9}$ with respect to horizontal axis	9.84°	0.22°
Orientation of $Link_{6,8}$ with respect to horizontal axis	-13.84°	0.63°
Orientation of $Link_{5,6}$ with respect to horizontal axis	-68.58°	-93.54°
Mass of a single CBW[2]	421 kg	344 kg
I_G[3] of a single CBW	10.6 kg×m^2	9.4 kg×m^2
c.m. of the LH CBW (in mm)	(-432.1,-32.5, 0.0)	(-428.4,8.6, 0.0)
c.m. of the RH CBW (in mm)	(441.4, -33.3,0.0)	(437.5, 9.4, 0.0)
$l_{15,17}$	128 mm	129 mm
$l_{15,16}$: $l_{16,17}$	28 mm : 100 mm	27 mm : 102 mm

[1]Stroke : Distance between top dead center and bottom dead center of the slide
[2]CBW : Counterbalance weight
[3]IG : Centroidal mass moment of inertia about an axis passing through mass center

The conditions prescribed in (1) and (2) are to make favorable phase relationships between the counterbalance weights and other major contributing links in order for the counterbalance weights to effectively counteract the dynamic unbalance.

In Table 2, the design parameters before and after dynamic balancing are compared. In Fig. 2 and Fig. 3, the accelerations and angular accelerations of some important links are compared during one revolution of the crankshaft in a time period of 0.05 sec before and after balancing work, respectively. The computed dynamic unbalance force and moment before and after dynamic balancing are compared in Fig. 4.

From Fig. 4 and Table 2, it is demonstrated that the orientation of $Link_{5,6}$ should be close to vertical, and those of $Link_{4,9}$ and $Link_{6,8}$ be close to horizontal when the orientation of the crankshaft is horizontal as shown in Fig. 1. This would be the primary condition leading to successful dynamic balancing. From Fig. 3, it can be found that even after balancing two counterbalance weights do not have identical accelerations and angular accelerations but have small differences. After balancing, the most pronounced feature is that the accelerations and angular accelerations of the mass centers of the counterbalance weights have nearly opposite

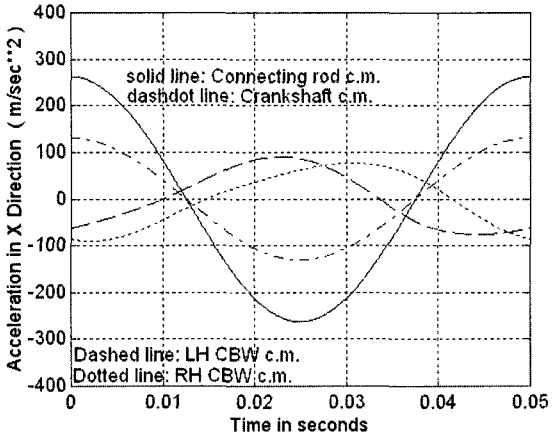

(a) Accelerations in X direction

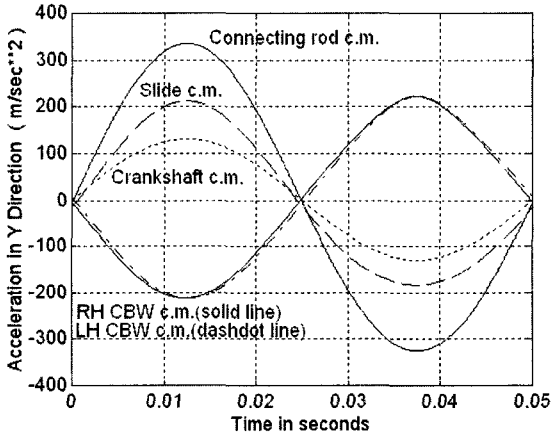

(b) Accelerations in Y direction

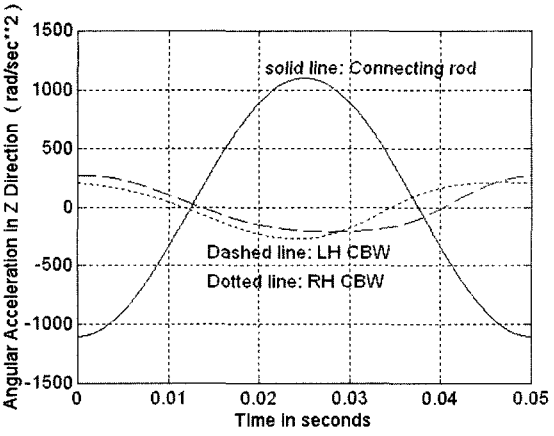

(c) Angular accelerations in Z direction

Fig. 2 Comparison of accelerations and angular accelerations before balancing (LH : left-hand, RH : right-hand, CBW : counter-balance weight)

phases when compared to those of crankshaft, connecting rod, slide, and slide column. The dynamic characteristics of the link motion mechanism change drastically when varying the design parameters for the links and constraint joints. For many possible combinations of design variations, dynamic simulations were carried out in search of the better combination reducing dynamic unbalance. The simulations using either Newtonian or Lagrangian mechanics produced identical results as expected. The dynamic unbalance contributed by slide, crankshaft, connecting rod, slide column are large since their accelerations of mass center and angular accelerations as well as their masses and centroidal mass moments of inertia have large values. In this work, for example, the values of mass for slide, crankshaft, connecting rod, and each slide column were 235 kg, 130 kg, 101 kg, 51 kg, respectively.

Considering dynamic unbalance force in Y direction, its first harmonic component could be almost removed but its second harmonic component still remained after balancing work as presented in Fig. 4. This second harmonic component can no longer be reduced by further dynamic balancing but by e.g. installing additional apparatuses on the mechanism which rotate with twice the rotational speed of the crankshaft.

Considering dynamic unbalance force in X direction and dynamic unbalance moment in Z direction, only the first harmonic component is dominant regardless of dynamic balancing work. In Table 3, maximum values of dynamic unbalance is compared before and after balancing work. It can be seen that drastic reduction of dynamic unbalance in a link motion mechanism is possible. In high-speed operation, the link motion mechanism exhibits high nonlinearities both in its kinematic and dynamic characteristics.

Dynamic unbalance in a link motion mechanism could be greatly reduced by properly designing a pair of counterbalance weights and other design parameters.

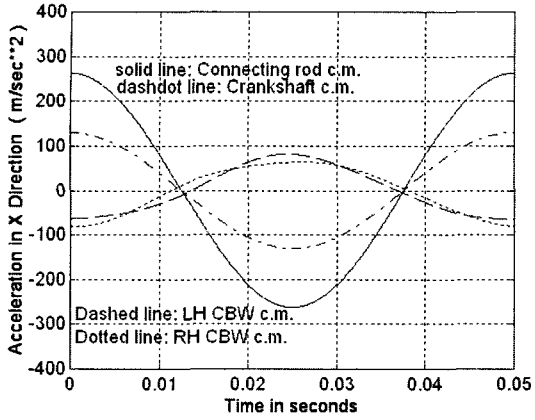

(a) Accelerations in X direction

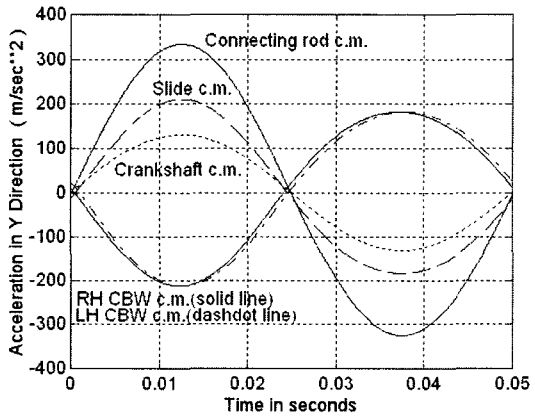

(b) Accelerations in Y direction

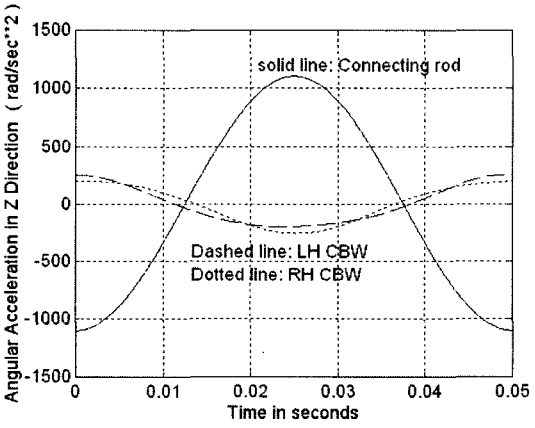

(c) Angular accelerations in Z direction

Fig. 3 Comparison of accelerations and angular accelerations after balancing(LH : left-hand, RH : right-hand, CBW : Counterbalance weight)

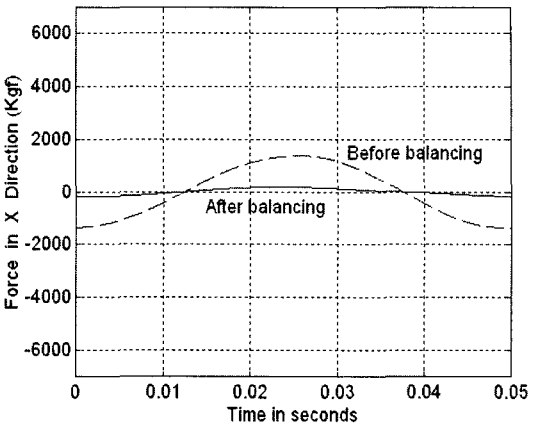

(a) Dynamic unbalance force in X Direction

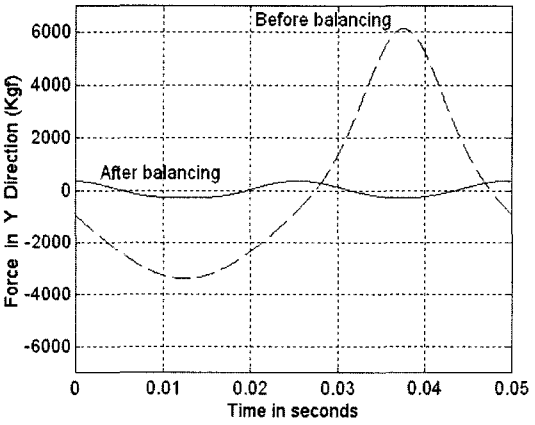

(b) Dynamic unbalance force in Y Direction

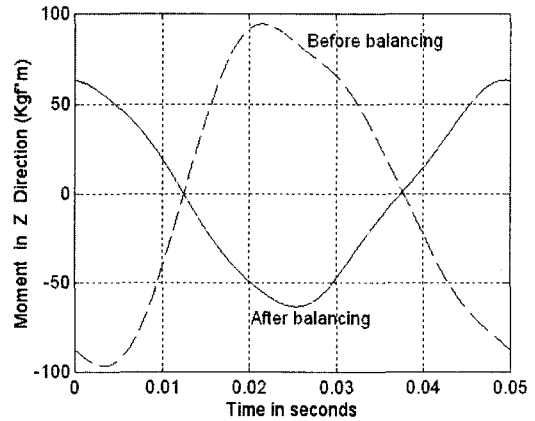

(c) Dynamic unbalance moment in Z Direction

Fig. 4 Dynamic unbalance force and moment before and after dynamic balancing

Table 3 Maximum dynamic unbalance force and moment before, after balancing

	Before balancing	After balancing
Max. unbalance force in X direction	1,370 Kgf	186 Kgf
Max. unbalance force in Y direction	6,142 Kgf	356 Kgf
Max. unbalance moment in Z direction	96 Kgf·m	63 Kgf·m

4. Conclusion

In this work, the methods for reducing dynamic unbalance in a link motion punch press were investigated by kinematic and dynamic analyses. The dynamic unbalance produced by a complicated and nonlinear link motion mechanism, which is executing constrained motions, could be substantially reduced.

Kinematic optimizations on some links were carried out in order for the counterbalance weights to counteract dynamic unbalance efficiently. The procedures for automating the model setup of the whole mechanism were presented to handle frequent design changes.

The resultant dynamic unbalance force and moment acting on the main frame were formulated by using both Newtonian mechanics and Lagrangian mechanics.

For various combinations of design variations, dynamic simulations were carried out in order to reduce dynamic unbalance.

References

(1) Berkof, R. S. and Lowen, G. G., 1969, "A New Method for completely Force Balancing Simple Linkages", ASME Journal of Engineering for Industry, Vol. 91, No. 1, series B, pp. 21~26.

(2) Berkof, R. S. and Lowen, G. G., 1971, 'Theory of Shaking Moment Optimization of Force-balanced 4-bar Linkages", ASME Journal of Engineering for Industry, Vol. 93, No. 1, series B, pp. 53~60.

(3) Bagci, C., 1979, "Shaking Force Balancing of Planar Linkages with Force Transmission Irregularities Using Balancing Idler Loops", Mechanism and Machine Theory, Vol. 14, No. 4, pp. 267~284.

(4) Lowen, G. G., Tepper, F. R. and Berkof, R. S., 1983, "Balancing of Linkages-An Update", Mechanism and Machine Theory, Vol. 18, No. 3, pp. 213~220.

(5) Kochev, I., 1987, "General Method for Full Force Balancing of Spatial and Planar Linkages by Internal Mass Redistribution", Mechanism and Machine Theory, Vol. 22, No. 4, pp. 333~341.

(6) Streit, D., and Gilmore, B., 2005, "Perfect Spring Equilibrators for Rotatable Bodies", ASME J. Mech., Transm., Autom. Des., Journal of Mechanical Design, Vol. 111, No. 4, pp. 451~458.

(7) Gosselin, C. M. and Zhang W. J., 1999, "Static Balancing of 3-DOF Parallel Mechanism and Manipulators", Int. J. Robot. Res., Vol. 18, No. 8, pp. 819~829.

(8) Eber-Uphoff, I., Gosselin, C. M. and Laliberte, T., 2000, "Static Balancing of Spatial Parallel Platform Mechanisms-revisited", Journal of Mechanical Design, Vol. 122, No. 1, pp. 43~51.

(9) Kobayashi, K., 2001, "Comparison between Spring Balancer and Gravity Balancer in Inertia Force and Performance", Journal of Mechanical Design, Vol. 123, No. 4, pp. 549~555.

(10) Arakelian, V. H. and Smith, M. R., 2005, "Shanking Force and Shaking Moment Balancing of Mechanisms: A Historical Review With New Examples", Journal of Mechanical Design, Vol. 127, pp. 334~339.

(11) Ouyang, P. R. and Zhang W. J., 2005, "Force Balancing of Robotic Mechanisms Based on Adjustment of Kinematic Parameters", Journal of Mechanical Design, Vol. 127, pp. 433~440.

(12) Kim, C., Lee. B., Kim, D. and Jung, I., 2005,

"Element Design of Balancing Shaft for Reducing the Vibration in Engine Module", Transactions of the Korean Society for Noise and Vibration Engineering, Vol. 15, No. 11, pp. 1268~1275.

(13) Shabana, A. A., 1998, Dynamics of Multibody Systems, 2nd edn., Cambridge University Press, United Kingdom.

(14) Wasfy, P. R. and Noor, A. K., 2003, "Computational Strategies for Flexible Multibody Systems", Applied Mechanics Reviews, Vol. 56, No. 6, pp. 553~613.

(15) Vetyukov, YU., Gerstmayr J. and Irschik H., 2006, "Modeling Spatial Motion of 3D Deformable Multibody Systems with Nonlinearities", Multibody System Dynamics, Vol. 15, No. 1, pp. 67~84.

(16) Alshaer, B. J., Nagarajan, H., Beheshti, H. K., Lankarani, H. M. and Shivaswamy, S., 2005, "Dynamics of a Multibody Mechanical System with Lubricated Long Journal Bearings", Journal of Mechanical Design, Vol. 127, pp. 493~498.

(17) Flores, P., Ambrosio, J., Claro, J. C. P. and Lankarani, H. M., 2006, "Dynamics of Multibody Systems with Spherical Clearance Joints", Journal of Computational and Nonlinear Dynamics, Vol. 1, No. 3, pp. 240~247.

(18) Kolovsky, M. Z., Evgrafov, A. N., Semenov, Yu. A. and Slousch, A.V., 2000, Advanced Theory of Mechanisms and Machines, Springer-Verlag, Berlin.

(19) Shabana, A. A., 2001, Computational Dynamics, 2nd edn., John Wiley & Sons, Inc., New York.

(20) Rivin, E. I., 2003, Passive Vibration Isolation, ASME Press, New York.